



INVESTIGATION AND MODIFICATION OF AERODYNAMIC CHARACTERISTICS OF SUPERSONIC AIRCRAFT

Dr. Jafar M. Hassan

Department of Mechanical Engineering
University of Technology
Baghdad, Iraq, P.O. Box :35010

Dr. Laith K. Abbass

Department of Technical Education
University of Technology
Baghdad, Iraq, P.O. Box :35010
E-mail: laithabbass@yahoo.com

Eng. Laith W. Ismail

Center of Training and workshops
University of Technology
Baghdad, Iraq, P.O. Box :35010

الخلاصة:-

زيادة الكفاءة الأيروديناميكية مع ضمان المناورة الخارقة للطائرة ذات السرعة فوق الصوتية (F-16A) يتم تقديمها. الخواص الأيروديناميكية, توزيع الضغط على سطح الطائرة وأعلى رفع يتم حسابه للشكل الرئيسي للطائرة لأعداد ماخ وزوايا هجوم مختلفة في حالة الطيران تحت وفوق الصوتي, باستخدام طريقة الأشرطة (Panel Method) والمعادلات شبه التجريبية (DATCOM).

تم بناء برنامج حاسوبي فرض فيه آلية الدفع الموجه (TVFC) مع أسطح السيطرة (Canards), النتائج بينت أن أسطح السيطرة مع آلية الدفع الموجه قد ولدت عزم ترجح (Nose-down pitching moment) يستطيع إسناد الذيل الأفقي في حالة المناورات العالية. أما من الناحية الأيروديناميكية فإن (5-6%) زيادة في الكفاءة الأيروديناميكية وجدت بعد إضافة أسطح السيطرة عن الشكل الأصلي للطائرة في حالة الطيران تحت وفوق الصوتي.

ABSTRACT

Increasing the aerodynamic efficiency and enhancing the supermaneuverability for the selected supersonic aircraft (F-16A) is presented. Aerodynamic characteristics, surface pressure distribution and maximum lift are estimated for the baseline configuration for different Mach number and angles of attack in subsonic and supersonic potential flow, using a low order three-dimensional panel method supported with semi-empirical formulas of Datcom.

Estimation of the total nose-up and nose-down pitching moments about the center of gravity of the completed aircraft in subsonic region depending on the flight conditions and aircraft performance limitations. A modern program was implemented by suggesting a two dimensional thrust vectoring technique (pitch vectoring up and down) controlled by the best design of advanced aerodynamic and control surface (foreplane or canard). Work results shows that the canard (as a control surface) with thrust vectoring produces enough nose-down moment and can support the stabilator at high maneuvers, while for an aerodynamic surface, a rate of (5-6%) increase was achieved in the aerodynamic efficiency (lift-to-drag ratio) of the baseline configuration in both subsonic and supersonic flight.

NOMENCLATURE

| | | |
|-----------------|--|---------------------|
| A_i | Panel area | m ² |
| AR | Lifting surface aspect ratio | - |
| b | Lifting surface span | m |
| c | Lifting surface chord | m |
| c_{avg} | Mean geometric chord of the wing | m |
| C_D | Drag coefficient | - |
| C_{D0} | Drag coefficient at zero lift (parasite drag coefficient) | - |
| C_L | Lift coefficient | - |
| C_L^α | Lift curve slope | 1/deg |
| C_i^α | Airfoil two dimensional lift curve slope | 1/deg |
| C_M | Pitching moment coefficient | - |
| $C_{M cg}$ | Pitching moment coefficient about the center of gravity | - |
| C_{M0} | Pitching moment coefficient at zero angle of attack | - |
| C_N | Normal force coefficient | - |
| C_P | Pressure coefficient | - |
| C_T | Tangential force coefficient | - |
| g | Aircraft load factor | - |
| l_c | Distance from the wing's quarter chord to the canard's quarter chord | m |
| l_h | Distance from the quarter chord point of the average chord of the main wing to the quarter average chord point on the horizontal surface in subsonic speed | m |
| M_i | Pitching moment about the origin of panel i | - |
| M_∞ | Free stream Mach number | - |
| N_i | Normal force of panel I | N |
| q_i | Resultant velocity at panel i | m/s |
| S | Lifting surface reference area | m ² |
| T_i | Tangential force of panel i | N |
| T | Engine thrust | N |
| u_i, v_i, w_i | Components of the velocity at panel i in x, y and z coordinates | m/s |
| V | Stream velocity | m/s |
| W | Aircraft weight | N |
| x_i, y_i, z_i | Coordinates of the panel control point | m |
| z_h | Vertical distance of the horizontal surface above the plane of the main wing | m |
| α | Angle of attack | deg. |
| θ | Inclined angle for the panel with respect to y-direction | |
| β^2 | Compressibility parameter = $\sqrt{1 - M^2}$ or $\sqrt{M^2 - 1}$ | deg. |
| γ | Singularity strength | M ³ /s.m |
| δ | Inclined angle for the panel with respect to x-direction | deg. |
| δ_c | Deflection angle of the canard | deg. |



| | | |
|--|--|-------------------|
| δ_s | Deflection angle of the horizontal tail (Stabilator) | deg. |
| δ_{TV} | Deflection angle of the thrust vectoring | deg. |
| ε | Downwash angle | deg. |
| ε_u | Upwash angle | deg. |
| $\frac{\partial \varepsilon}{\partial \alpha}$ | Rate of downwash | - |
| $\frac{\partial \varepsilon_u}{\partial \alpha}$ | Rate of upwash | - |
| ρ | Air density | kg/m ³ |
| λ | Taper ratio | - |
| ϕ | Velocity potential | m/s |

INTRODUCTION

the emphasis today is on technology that will allow fighters to survive and win in combat. There is great interest today in an area of technology that goes under the generic title of “Supermaneuverability”.

Dr. Herbst, of West Germany’s Messerschmitt-Bo1kow-Blohm [Col. William, 1988], defined supermaneuverability as the capability to execute maneuvers with controlled sideslip at angles of attack well beyond those for maximum lift. The designer-general of the Sukhoi “Mikhail Simonov” defined the supermaneuverability [Venik’s Aviation, 2002], as a fighter’s capacity to turn toward its target from any position in space with at least twice the rate of turn that the enemy fighter is capable of. One method to enhance maneuvering is to simply use all lift inherent in a particular design, or increasing the aerodynamic efficiency (Lift/Drag). Another way of obtaining unconventional maneuvering especially at slow speeds and at high angles of attack is the addition of Thrust Vectoring Flight Control (TVFC) at the rear (i.e. changing the direction of the thrust produced by an aircraft’s engine(s) (Fig. 1), and the foreplan (Canard) which provides substantial lift as well as longitudinal trim and control and the control canard which is used for longitudinal trim and control only (Fig. 2). In the present paper, Depending on the flight condition requirements during pull-up maneuver and with assistance of panel method program and developed programs, a foreplane (canard) surface has been designed (geometry, position, permissible deflection angle) using the iterative process and added to the model for two purposes, as an aerodynamic surface and as a control surface with thrust vectoring technique. Studying the effect of the canard surface on the aerodynamic efficiency and total pitching moment of the whole configuration.

COMPUTATIONAL AERODYNAMIC ANALYSIS [Mason, 1998]

For small perturbations, the governing equation of the potential flow can be simplified greatly and solution of many problems becomes possible. The linearized three-dimensional potential equation is [L. Morino, 1974]:

$$\beta^2 \phi_{xx} + \phi_{yy} + \phi_{zz} = 0.0 \quad (1)$$

Where β^2 is the compressibility parameter and depends upon Mach number. Expect for the case of the transonic flow, Eq.1 is valid for both subsonic ($\beta^2 = (1 - M_\infty^2)$) and supersonic flows ($\beta^2 = (M_\infty^2 - 1)$).

The pressure coefficient is then calculated using the exact isentropic formula

$$C_{p_i} = \frac{-2}{\gamma M_\infty^2} \left\{ \left[1 + \frac{\gamma-1}{2} M_\infty^2 (1 - q_i^2) \right]^{3.5} - 1 \right\} \quad (2)$$

$$\text{where } q_i^2 = u_i^2 + v_i^2 + w_i^2 \quad (3)$$

The forces and moments acting on the configuration can then be calculated by numerical integration.

$$N_i = -A_i C_{p_i} \cos \theta_i \cos \delta_i \quad (4)$$

$$T_i = A_i C_{p_i} \sin \delta_i \quad (5)$$

$$M_i = N_i x_i - T_i z_i \quad (6)$$

The forces and moment coefficients acting on the configuration are obtained by summing the panel forces and moments on both side of the plane of symmetry.

$$C_N = \frac{1}{S} \sum_{i=1}^N 2^* N_i \quad (7)$$

$$C_T = \frac{1}{S} \sum_{i=1}^N 2^* T_i \quad (8)$$

$$C_M = \frac{1}{S \bar{c}} \sum_{i=1}^N 2^* M_i \quad (9)$$

The lift and drag coefficients formulas are:-

$$C_L = C_N \cos \alpha - C_T \sin \alpha \quad \text{for (wing-body)} \quad (10)$$

$$C_D = C_N \sin \alpha + C_T \cos \alpha \quad \text{for (wing-body-tail)} \quad (11)$$

The maximum lift coefficient of lifting surfaces at subsonic speed is given by:

$$C_{L_{\max}} = (C_{L_{\max}})_{\text{base}} + \Delta C_{L_{\max}} \quad (12)$$

The value of $(C_{L_{\max}})$ and $\Delta C_{L_{\max}}$ can be estimated from [(Hoak.), (Daniel, 1992)].

Taking into the considerations the contributions of the additional horizontal lifting and stabilizer surfaces on the aircraft total lift curve slope, to determine a horizontal tail contribution (the rate of downwash) [Fink, 1975]:-

$$\frac{\partial \varepsilon}{\partial \alpha} = \frac{21^\circ C_L^\alpha}{AR^{0.725}} \left(\frac{c_{avg}}{l_h} \right) \left(\frac{10-3\lambda}{7} \right) \left(1 - \frac{z_h}{b} \right) \quad (13)$$

Where $\frac{\partial \varepsilon}{\partial \alpha}$ is the rate of change of downwash in angle of attack.

$$\Delta C_L^\alpha \text{ (due to horizontal tail)} = C_{L_t}^\alpha \left(1 - \frac{\partial \varepsilon}{\partial \alpha} \right) \frac{S_t}{S} \quad (14)$$

While the contributions of the additional horizontal lifting surface (Canard) to the aircraft (the rate of upwash) is:-



$$\frac{\partial \varepsilon_u}{\partial \alpha} = (0.3AR^{0.3} - 0.33) \left(\frac{l_c}{c}\right)^{-\left(1.04 + 6AR^{-1.7}\right)} \tag{15}$$

Where $\frac{\partial \varepsilon_u}{\partial \alpha}$ is the rate of change of upwash in angle of attack.

$$\Delta C_L^\alpha \text{ (due to canard)} = C_{Lc}^\alpha \left(1 + \frac{\partial \varepsilon_u}{\partial \alpha}\right) \frac{S_c}{S} \tag{16}$$

Once the contributions of canard and horizontal tail are estimated, the whole aircraft lift curve slope is given by:

$$\begin{aligned} C_L^\alpha \text{ (Total aircraft)} = & C_L^\alpha \text{ (wing+body+strake)} + \\ & \Delta C_L^\alpha \text{ (due to horizontal tail)} + \\ & \Delta C_L^\alpha \text{ (due to canard)} \end{aligned} \tag{17}$$

TOTAL PITCHING MOMENT COEFFICIENT [(F-15,2003),(Shaker,2000), (John,1997),(Perkins,1949),(B. Etkin,1996),(Nelson,1998)]

For longitudinal static stability and pitch control, the total aircraft pitching moment curve is only considered. However, it is of interest to know the contribution of the wing, fuselage, tail, propulsion system, etc., to the pitching moment and longitudinal static stability characteristics of the aircraft. The aircraft pitching moment coefficient about the center of gravity due to the contribution of wing-fuselage, aft tail, canard and thrust vectoring is:-

$$C_{M_{cg}} = C_{M_0} + C_{M_\alpha} \alpha + C_{M_{\delta_S}} \delta_S + C_{M_{\delta_c}} \delta_c + C_{M_{TV}} \tag{18}$$

g-LOADING [Kotelnikov ,1973]

In some cases to analyze the motion of the aircraft it is convenient to use the relative magnitudes of forces per unit of weight of the aircraft rather than the absolute ones. For this purpose the concept of the g-load is introduced. Aircraft load factor (g) or (g-loading) during a turn expresses the maneuvering (or acceleration due to lift) of an aircraft as a multiple of the standard acceleration due to gravity (g=9.81 m/s²). Therefore, it is related to turn. There are two important turns, “sustained” turn for some flight condition at which the thrust of the aircraft is just sufficient to maintain velocity and altitude in the turn i.e., thrust must equal the drag and lift equal g times the weight. Thus the maximum g for sustained turn can be expressed as [Daniel, 1992]:

$$g = \sqrt{\frac{0.5\rho V^2}{K(W/S)} \left(\frac{T}{W} - \frac{0.5\rho V^2 C_{D0}}{W/S} \right)} \tag{19}$$

where $K = 1/(\pi AR e)$, $e \approx 0.8 - 1.0$

The second turn is “instantaneous”, if the aircraft turns at a quicker rate; the drag becomes greater than the available thrust, so the aircraft begins to slow down or loss altitude. Therefore, g

will be limited by the maximum lift coefficient or structural strength of the aircraft and is equal to [Daniel, 1992]:

$$g = \frac{0.5\rho V^2 SC_{Lmax}}{W} \quad (20)$$

VERIFICATION TEST

For aerodynamic analysis, the verification test was used to confirm the validity of the computer program results with the flight data of supersonic aircraft model (Sukhoi Cy-20). Three-dimensional paneling of the symmetrical model contain three parts. 14 strips along the fuselage length and 6 strips along the half meridian have been used to represent the body fuselage by forming 84 panels. 12 strips along the span and 8 strips in each contour line at chordwise direction were used for wing, horizontal tail and vertical tail, which made 288 panels. Therefore, the total number of panels is 372 panels.

Using the above inputs with the assistance of theoretical approach computations for the lift and drag coefficients on the complete surface were made in three stages, wing-body, stabilizer-body and fin-body. (Table 1) gives the comparison results between the computer program and flight test [AIRCRAFT,1972].

A good correlation was obtained although there was about +8% error in lift computations at supersonic speed. In fact, the present code shows a good performance in the subsonic region and an acceptable duration in the supersonic region. The maximum Mach number and angle of attack depends on the shape and dimension of the configuration, and should be within the linear aerodynamic zone.

RESULTS AND DISCUSSION

Three-dimensional mesh and contours plotting were used to represent the pressure distribution over the complete selected aircraft configuration. (Fig. 3) represent these distributions at Mach number 0.8 and 1.6 with effective angles of attack of 10 and 15 degrees.

The maximum contour distribution as shown in (Fig. 3(A)) at 0.8 Mach number is at the wing leading edge. It increases significantly when angle of attack is high. In (Fig. 3(A)), the Mach cone angle is approximately equal to the wing leading edge angle and covers the horizontal tail area when Mach number is 1.6 (Fig. 3(B)). The aircraft performance in cases of instantaneous and sustained maneuvers capability (load factor g) is shown in the form of contours (using the 3-dimensional Kriging Algorithm to represent the results [Kotelnikov,1973]). (Figs. 4 and 5) are used for specific flight conditions (constant combat weight = 12036.53 kg, different altitude = 0 m, 3048 m, 6069 m, 9144 m, 12192 m, 15240 m, Mach number up to 1.0, required angle of attack).

The maximum differences $\Delta C_{M c.g}$ between the two pitching moments generated from the two stabilator's deflection (positive and negative deflections $\pm 25^\circ$) is (0.1561) at an altitude of (6096 m) and Mach number (0.9) for (5g) in case of sustained maneuver, a (0.21452) was achieved at altitude (6096 m) and Mach number (0.9) for (7g). As for instantaneous maneuver, a (0.21452) was achieved at altitude (6096 m) and Mach number (0.9) for (7g). So, all the moving small foreplane (canard) surface, large and fast actuator and near to the aircraft nose with Thrust Vectoring Flight Control (TVFC) can be used to fix this problem.

Because both are sustained and instantaneous maneuvers $\Delta C_{M c.g \max}$ have the same altitude (6096 m) and Mach number (0.9), therefore, an intermediate value of $\Delta C_{M c.g \max}$



(≈ 0.18) will therefore be considered as an initial trail. Also to simplify the issue, the suggested canard will have the same airfoil section as for the wing and horizontal tail, i.e., NACA 64_A-204, pitching moment about aerodynamic center $C_{M a.c.}$ about (-0.02) and the two-dimensional lift curve slope c_l^α is approximately 0.1/deg [John,1997]. The conventional design procedure (or the computerized iterative process) was used to solve the problem. Designing the proper area, lift and position of the canard was considered in the first step. Results of the iterative process are shown in (Fig. 6) for the first step. The minimum canard area is favorable because it ensures minimum interference with the fuselage and wing. From (Fig. 6(A)), the proper lift curve slope C_{LC}^α can be chosen. The canard longitudinal position (Fig. 6(B)) is chosen to be as minimum as possible from aircraft nose to have a long arm for moment. Therefore, the required canard lift, area and position. At $\Delta C_{M c.g. \max} \approx 0.18$ Canard Area $\approx 0.070 \rightarrow 0.072$ of Wing Area $\approx 1.95 \rightarrow 2.0 \text{ m}^2$, Minimum required Canard Lift Curve Slope = 0.039/deg and the Longitudinal Canard Position from Aircraft Nose=3.7m. (Table 2) shows the initial canard layout which can be considered for the preliminary design.

The drag polar and lift-to-drag ratio of the isolated canard surface is plotted for different Mach numbers as shown in (Fig. 7). The maximum lift curve slope of isolated canard C_{LC}^α is 0.00432 /deg at 1.2 Mach number (Fig. 8). It appears as shown in (Fig. 9) that this model has enough moment and can support the horizontal tail (stabilator) during nose-down moment at high maneuvers capability. The effect of canard as an aerodynamic surface can be shown in (Figs. 10,11 and 12). In general, a 5-6% increase in the lift curve slope and lift-to-drag ratio of the baseline configuration in both subsonic and supersonic regimes has been achieved when using small, all moving canard surface.

CONCLUSIONS

- The pressure distributions over the upper surfaces of the configuration shows that the contour distribution increased significantly when the Mach number decreases and the pressure distribution shows a clear pattern of increasing peak pressure with angle of attack in agreement with the increasing the strength of the leading edge vortex.
- It appears that the selected supersonic aircraft was unstable in the subsonic aircraft regime (negative static margin) while, it was stable in the supersonic regime. Static margin is a measure of the aircraft stability, for stability criterion becomes when static margin > zero.

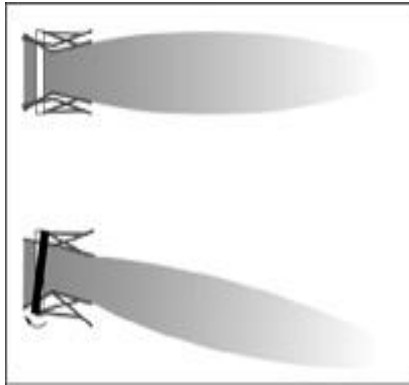


Figure 1
Thrust Vectoring Flight Control

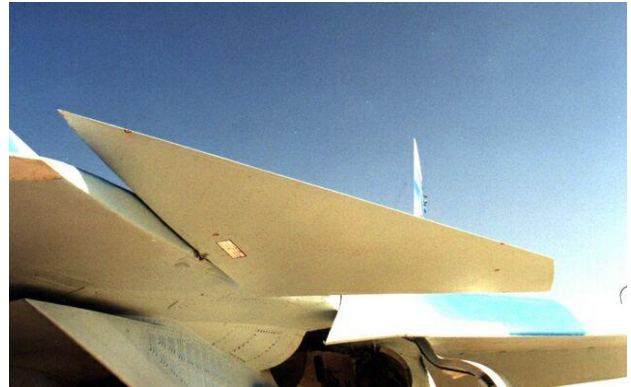


Figure 2
Foreplane (Canard)

Table 1
Cy-20 Aerodynamic Characteristics

| | Mach No. | Flight Data [15] | Wing-Body-Tail | | | | Error % |
|---------------------------|----------|------------------|----------------|----------------------|--------------------|---------|---------|
| | | | Wing/Body | Horizontal Tail/Body | Vertical Tail/Body | Total | |
| C_L^α / deg | 0.8 | 0.0541 | 0.047346 | 0.007043 | - | 0.05052 | -6.60 |
| | 1.3 | 0.0607 | 0.054233 | 0.009251 | - | 0.05745 | -5.35 |
| | 1.6 | 0.05123 | 0.052063 | 0.009147 | - | 0.05537 | +8.09 |
| C_{D0} | 0.8 | 0.0171 | 0.00867 | 0.00493 | 0.00256 | 0.01616 | -5.49 |
| | 1.3 | 0.0393 | 0.01859 | 0.01254 | 0.00708 | 0.03821 | -2.77 |
| | 1.6 | 0.0425 | 0.02625 | 0.01082 | 0.00584 | 0.04291 | +0.96 |

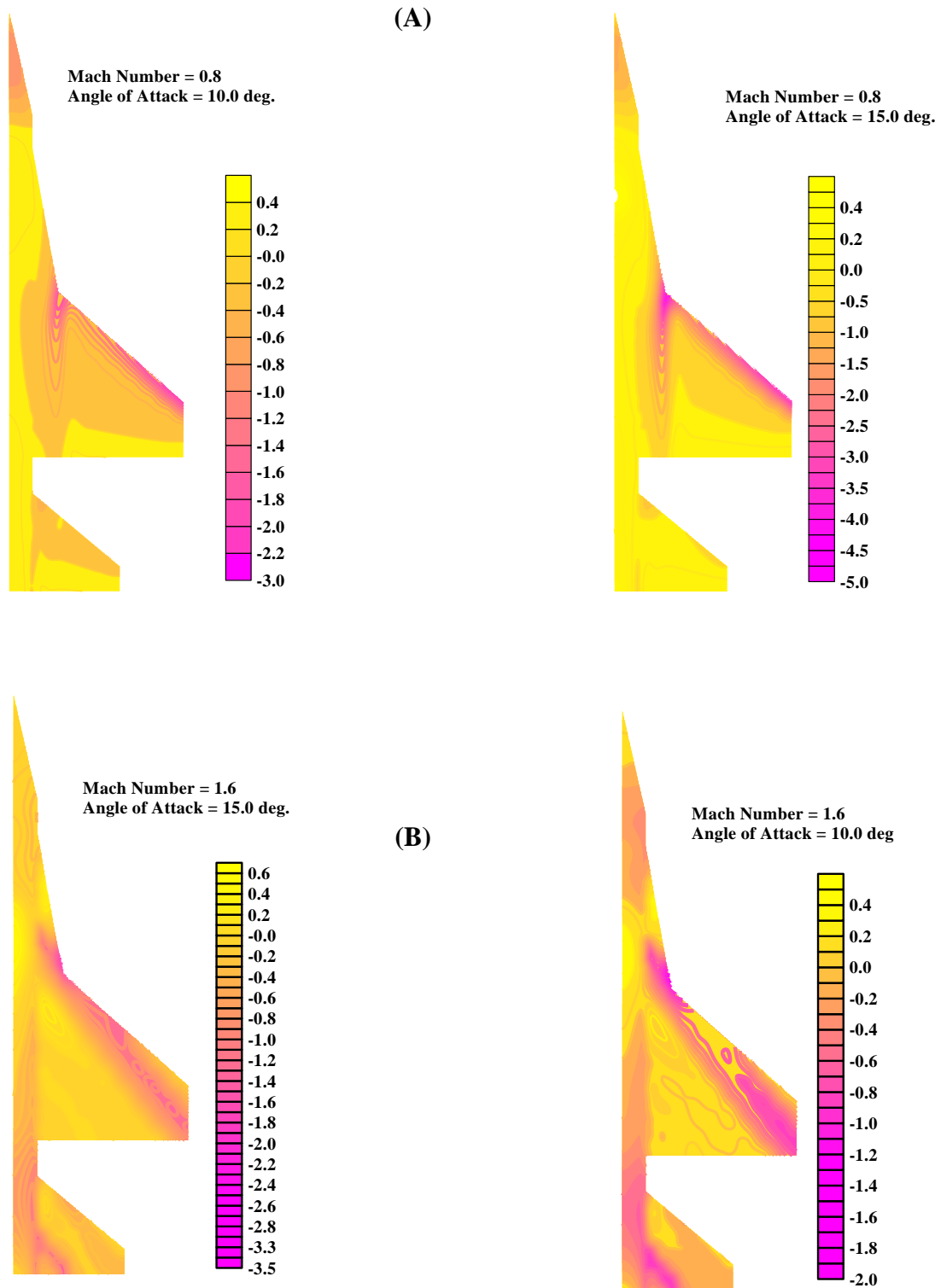


Figure 3
Pressure Distribution Contours on the Upper Surface at(0.8 & 1.6) Mach number for (10 & 15) Angle of Attack

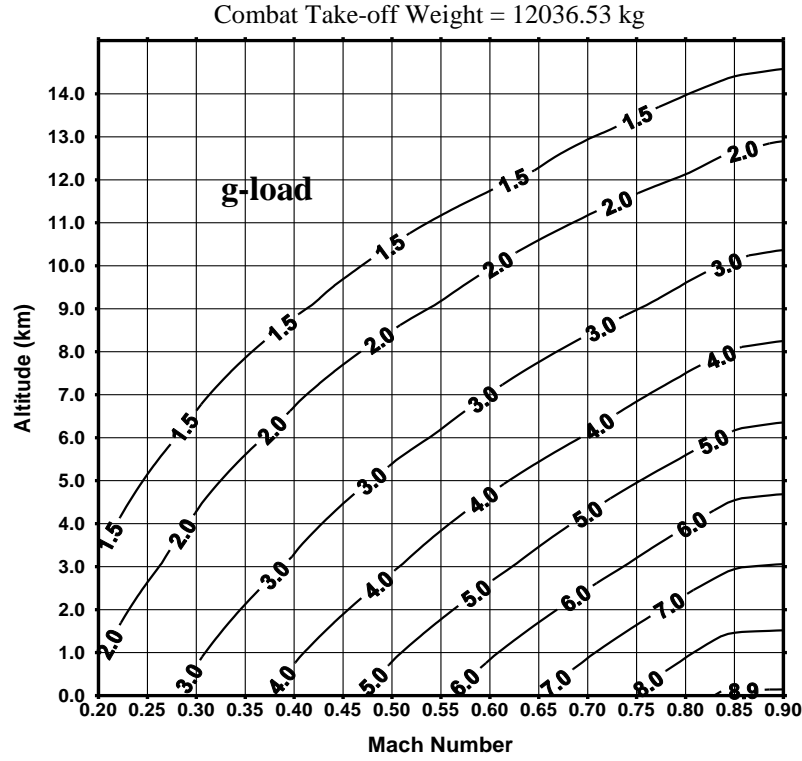


Figure 4
Sustained Maneuvers Capability of the Selected
Model in Subsonic Region

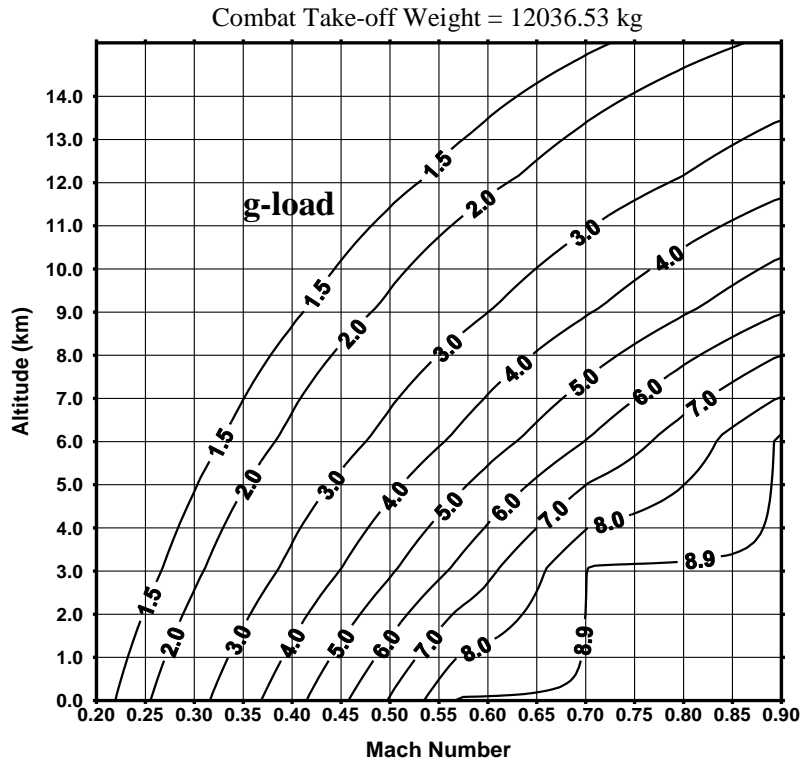


Figure 5
Instantaneous Maneuvers Capability of the Selected
Model in Subsonic Region

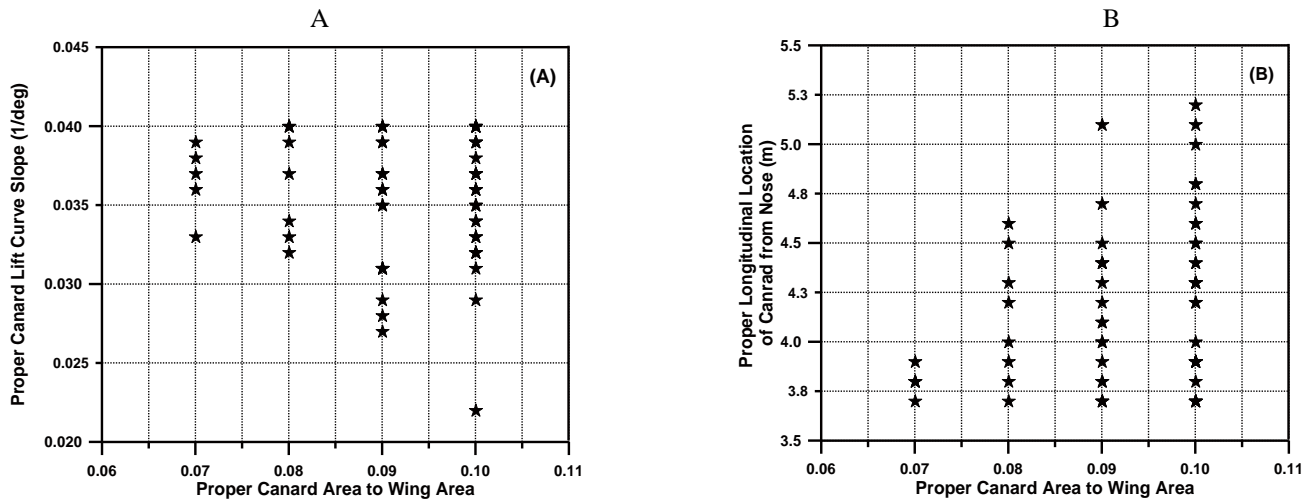


Figure 6
Proper Canard Lift Curve Slope (1/deg) and its Longitudinal Location from the Aircraft Nose
versus the Canard to Wing Area Ratio

Table 2
The Initial Canard Layout

| | |
|----------------------------|--------|
| Area (m ²) | 1.995 |
| Total Span (m) | 2.1 |
| Root Chord (m) | 1.6 |
| Tip Chord (m) | 0.3 |
| Aspect Ratio | 2.2105 |
| Taper Ratio | 0.1875 |
| Leading Edge Angle (deg.) | 57 |
| Trailing Edge Angle (deg.) | 73 |
| Maximum deflection (deg.) | ± 40 |

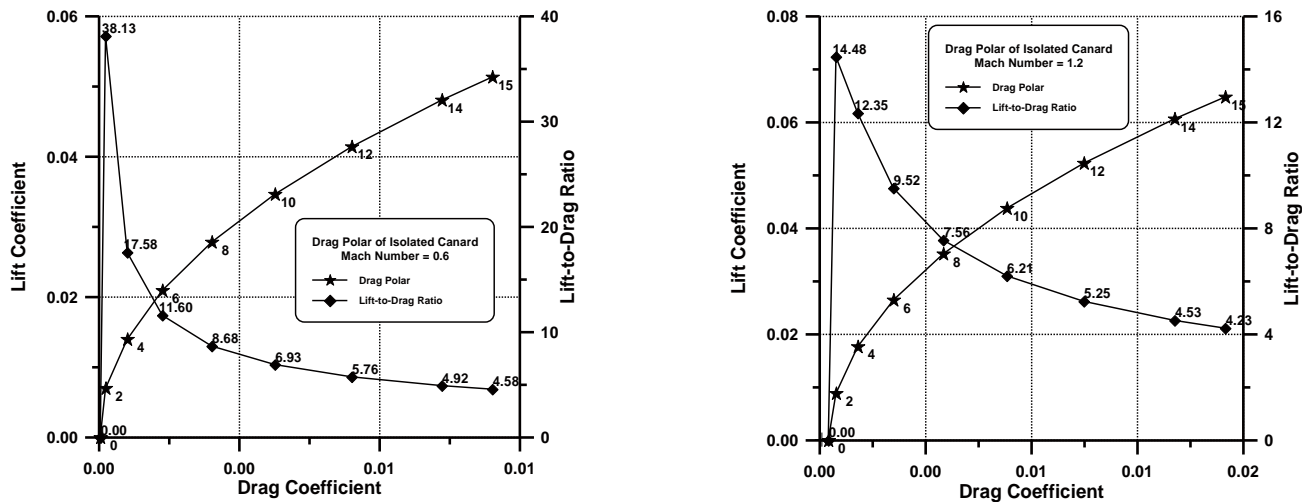


Figure 7
Drag Polar and Lift-to-Drag Ratio of Isolated Canard Surface
At Different Mach number

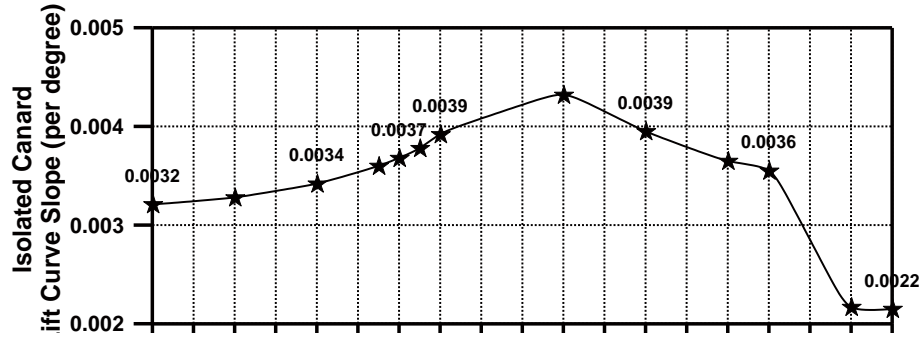


Figure 8
 Lift Curve Slope (per degree) of Isolated Canard Surface
 As a Function of Mach number

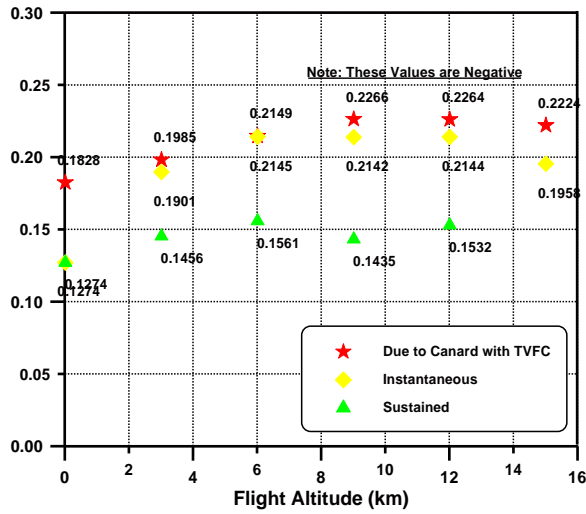


Figure 9
 Effect of Canard with TVFC Pitching Moment

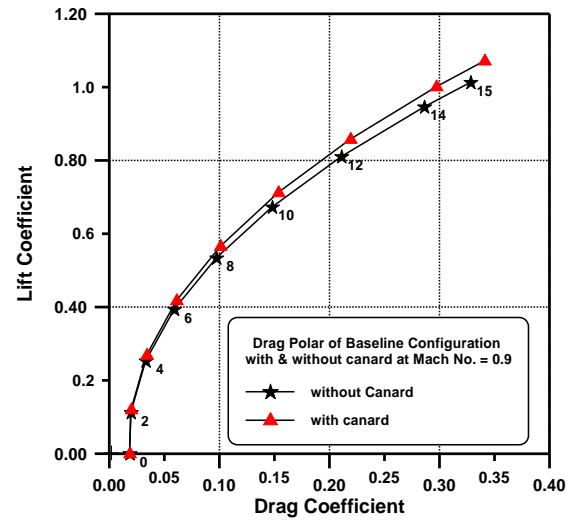


Figure 10
 Comparison Study of Drag Polar between the Baseline Configuration and Configuration with Canard Surface

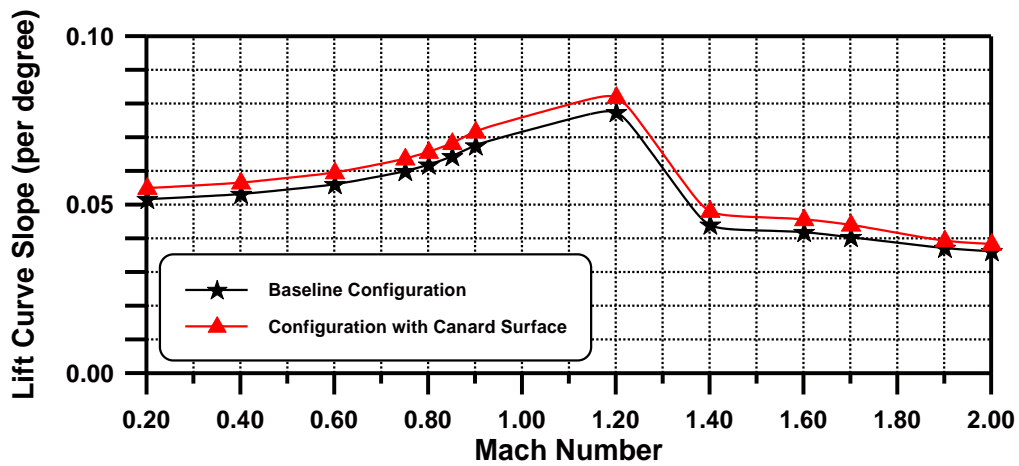


Figure 11
 Comparison Study of Lift Curve Slope between the Baseline Configuration and Configuration with Canard Surface

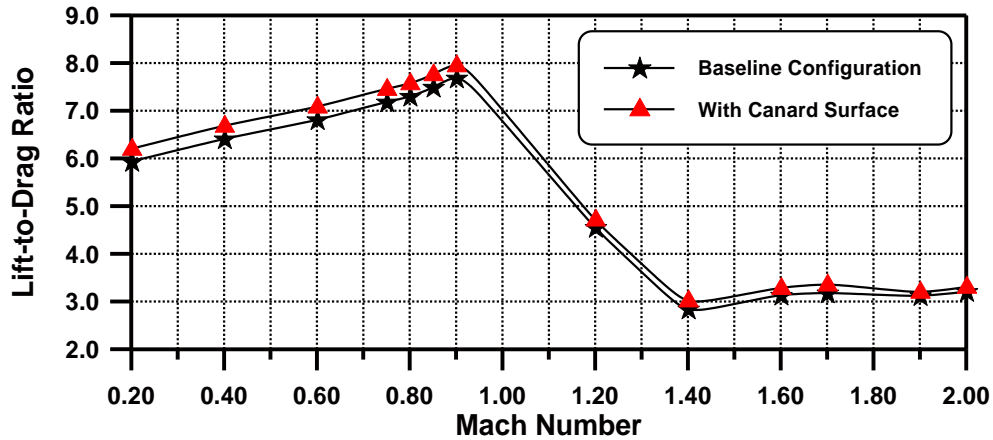


Figure 12
Comparison Study of Lift-to-Drag between the Baseline Configuration and Configuration with Canard Surface

REFERENCES

- AIRCRAFT Cy-20, Technical Description, BOOK 1, “GENERAL INFORMATION AND FLIGHT PERFORMANCE”, TOP SECRET, Copy No. 28, 1972.
- B. Etkin and L. D. Reid, “Dynamics of Flights: Stability and Control”, John Wiley & Sons, New York, NY, third edition, 1996.
- Col. William D. Siuru, Jr., “Supermaneuverability”, Aerospace Power Journal, Spring, 1988.
- Email: aspj@maxwell.af.mil
- Danie P. Raymer, “Aircraft Design: A Conceptual Design”, AIAA, 1992.
- Fink, R.D., “USAF Stability and Control DATCOM”, Wright-Patterson AFB, OH, 1975.
- “F-15 ACTIVE (Advanced Control Technology for Integrated Vehicles)- Research Program History and Technology”, Document: EG-2003-01-001-DFRC, NASA Dryden Flight Research Center, 2003.
- Hoak, D., Ellison, D., et al., “USAF DATCOM”, Air Force Flight Dynamics Lab., Wright-Patterson AFB, OH.
- John J. Bertin, Randall J. Stiles, and Steven A. Brandt, “Introduction to Aeronautics: A Design Perspective”, American Institute of Aeronautics and Astronautics, January 1997.
- Kotelnikov, G. N., “Airplane Aerodynamics”, Textbooks for Cadets of aircraft-Technician Officer Schools, Russia, 1973.
- L. Morino and C.C. Luo, “Subsonic Potential Aerodynamics for Complex Configurations. A General Theory”, AIAA Journal, Vol. 12, No. 2, February 1974.
- Mason, W. H., “Applied Computational Aerodynamics”, Internet Pages (a PDF File), April 1998.

- Nelson, R. C., “Flight Stability and Automatic Control”, WCB McGraw-Hill, New York, NY, second edition, 1998.
- Perkins, D. Courtland and Hage, E. Robert, “Airplane Performance Stability and Control”, John Wiley & Sons, New York, NY, 1949.
- Shaker M. Hussain, “Flight Performance Optimization of Supersonic General Aviation Design”, Ph.D. Thesis, Military College of Engineering, Baghdad, 2000.
- Venik’s Aviation, “Breakthrough in Supermaneuverability”, June 19,2002.
- Email: www.aeronautics.ru/venik.way.to